EurJOC
European Journal of Organic Chemistry

Research Article
doi.org/10.1002/ejoc.202300227

Chemistry Europe
European Chemical Societies Publishing

www.eurjoc.org

Cargo Encapsulation in Photochromic Supramolecular Hydrogels Depends on Specific Guest-Gelator Supramolecular Interactions

Fabian Hoffmann,[a] Anna-Lena Leistner,[b] Susanne Kirchner,[b] Burkhard Luy,[a] Claudia Muhle-Goll,*[a] and Zbigniew Pianowski*[b, c]

Photochromic supramolecular hydrogels are prospective materials for light-triggered drug release and bionanotechnology. Here we present a structural analysis of peptide-derived photochromic supramolecular hydrogels, which were physically loaded with a selection of biologically related compounds, using advanced techniques of nuclear magnetic resonance. The results enable detailed and correct understanding of the loading process and will allow for correct design of pharmacologically relevant systems for phototriggered drug delivery.

Introduction

Stimuli-responsive materials play an increasingly important role in precisely controlled delivery of sensitive or potent therapeutic agents.[1] Visible light is a particularly favorable stimulus for such applications, as it is non-toxic, biorthogonal, and enables precise spatiotemporal control of the release process in vivo.[2] One of the most potent tools that enable transformation of light energy into microscopic and macroscopic effects are molecular photoswitches.[3] These compounds undergo reversible light-induced transformations of various nature – comprising *E/Z*-isomerizations, electrocyclizations, tautomerizations, bond formation and cleaving – upon irradiation with a particular frequency of light, characteristic for the given scaffold.[4] One typical consequence of these changes is photochromism – reversible color change upon exposure to light.[5] Well-known photochromic scaffolds encompass azobenzenes,[6] diarylethenes[7] or spiropyrans.[8] Their palette has been recently extended with new scaffolds,[9] including arylhydrazones,[10] indigoids,[11] donor-acceptor Stenhouse adducts,[12] or hemipiperazines.[13]

Molecular photoswitches have been merged with variable gelator motifs and produced a range of light-responsive hydrogels.[14] They have been successfully used in vitro for photocontrolled release of drugs, biopolymers and other bioactive substances.[15] Among them, one of our groups recently introduced a family of cyclic dipeptide-based low-MW hydrogelators containing azobenzenes.[16] They were physically loaded with oligonucleotides,[16a] proteins, and low-MW drugs (antimicrobial, anti-inflammatory and anticancer).[17] Upon irradiation (with UV,[16a,18] and later with more biocompatible visible light[19]), the hydrogels dissipated to fluids with concomitant release of the unmodified cargo to the surrounding aqueous solutions.

We have previously observed[17] that the investigated cargo types have variable rates of diffusion from the hydrogel in absence of irradiation ("leaking"). A crucial issue for understanding the integrity of our materials, and their potential applicability for pharmacologically feasible drug-delivery systems is how the cargo interacts with the gelator. Structural analysis of the non-irradiated materials with electron microscopy revealed the existence of an extensive network of supramolecular fibers formed by the gelator molecules.[17] The cargo presumably locates itself in cavities between the fibers. However, due to the small size it could not be properly visualized or identified in the electron microscopy experiments. Thus, we resorted to NMR spectroscopy, which is one of the most sensitive tools in the detection of molecule interactions. It is applicable over a wide range of affinities without requiring specific modifications. Moreover, its rich spectral information allows to generate atomic level details about the investigated interactions. Advanced NMR techniques (solid- as well as solution-state) have been applied to study supramolecular interactions in numerous sol-gel systems, including hydrogels composed of amino acids,[20] urea derivatives,[21] glycoconjugates,[22] as well as more complex compositions based on cyclodextrin binding to small hydrophobic residues.[23]

[a] F. Hoffmann, Prof. Dr. B. Luy, Dr. C. Muhle-Goll
Institute for Biological Interfaces 4
Karlsruhe Institute of Technology KIT
P.O. Box 3640
76021 Karlsruhe (Germany)
E-mail: claudia.muhle-goll@kit.edu
[b] Dr. A.-L. Leistner, Dr. S. Kirchner, Dr. Z. Pianowski
Institute of Organic Chemistry
Karlsruhe Institute of Technology KIT
Fritz-Haber-Weg 6
76131 Karlsruhe (Germany)
E-mail: pianowski@kit.edu
[c] Dr. Z. Pianowski
Institute of Biological and Chemical Systems – FMS
Karlsruhe Institute of Technology KIT
Hermann-von-Helmholtz-Platz 1
76344 Eggenstein-Leopoldshafen (Germany)

Supporting information for this article is available on the WWW under https://doi.org/10.1002/ejoc.202300227

Research Article
doi.org/10.1002/ejoc.202300227

The antibacterial ciprofloxacin, anti-inflammatory drugs (naproxen, diclofenac), anticancer drugs (actinomycin D) and a protein (cytochrome C) have been previously used as cargo.[17] Yet, the rate of cargo leaking in darkness did not correlate with their sizes – a large protein cytochrome C (>12000 Da) was diffusing out of the gel faster than naproxen and diclofenac (both below 300 Da), with the ciprofloxacin leaking rate located in between. Based on these observations, we hypothesized that the diffusion rate in absence of irradiation is only weakly related to the pore size between the hydrogel's fibers. Instead, the decisive factor in this case could be supramolecular interactions of the cargo with surrounding hydrogelator molecules (**1**). The hydrogelator **1** possesses an expanded aromatic system prone to hydrophobic interactions and π–π stacking, appended with a basic side chain of the lysine rest, which in turn can set ion pairs and polar interactions. In this report, we present detailed characterization of the gelator-cargo interactions for three selected guest compounds. To compare the influence of supramolecular interactions on the material assembly, we have chosen here three low-MW guest molecules: glucose **2** (180 Da) with a set of polar non-charged groups, the previously used ciprofloxacin **3** (331 Da) with polar groups and an aromatic system, and finally sodium cholate **4** (430 Da) with a polar acidic group and a hydrophobic steroid system (Figure 1). The results enable us to understand the whole system and optimize the structures of future bioactive guests in order to minimize the unwanted leaking process that hampers selectivity of the light-triggered delivery.

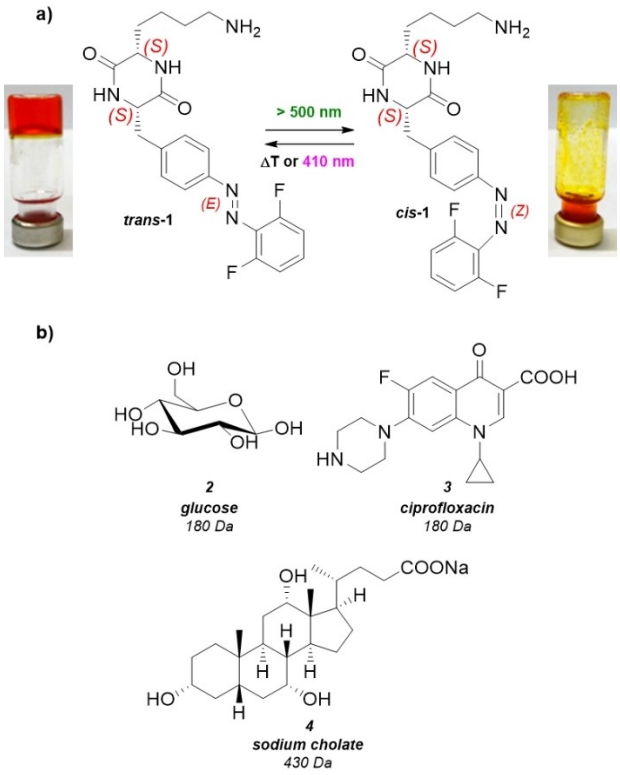

Figure 1. a) Photochromic supramolecular hydrogelator **1** can be mutually photoisomerized with green and violet light, which liquefies and reconstitutes the hydrogel, respectively ; b) hydrogels loaded with glucose **2**, ciprofloxacin **3**, and sodium cholate **4** are subjects of the current investigation.

We have selected the three particular cargo molecules, as they illustrate properly a set of different interactions that we consider important for our supramolecular system. Out of the other previously tested guest molecules,[17] naproxen and diclofenac due to their low water solubility (<100 μM) could not be properly characterized by NMR methods in presence of high concentrations of the gelator (40 mM), while cytochrome C due to its complex structure would lead to crowded spectra where single peaks between gelator and guest molecule cannot be discerned.

Results and Discussion

The hydrogels have been prepared according to the earlier established protocol from a freshly synthesized hydrogelator (see Supporting Information, pages S2–S9).[17] The chemical shift assignments of all components investigated in our systems were taken from previous publications (**1**[17] and **3**[24]) or the Biological Magnetic Resonance Databank[25] entries (doi:10.13018/BMSE000855 for **2** and doi:10.13018/BMSE000650 for **4**), and were confirmed with COSY and TOCSY spectra. The guest molecules have been loaded into the photochromic supramolecular hydrogel samples using the procedure described below (see the experimental section, Supporting Information page S10, and Table S2).

We used 1D selective NOESY, 2D NOESY and diffusion ordered spectroscopy (DOSY) spectra to assess the interactions between gelator **1** and respective guest molecules **2**–**4**. In general, NOESY spectra reveal an interaction between two nuclei that are close in space (<5 Å). These cross peaks stem from the nuclear Overhauser effect (NOE), a dipole-dipole cross relaxation through space. Whereas intramolecular cross peaks indicate steric relations between the inquired atoms, and thus enable correct chemical shift assignment within complex molecules, intermolecular cross peaks show that interactions between two molecules take place.

NOESY spectra of the isolated gelator and cargo molecules

The sign of an NOE depends on the molecular rotational tumbling time, which in turn depends on the molecular size and on the viscosity of the sample. Small molecules have a positive NOE, discernible in the selective 1D NOESY. In a 2D NOESY, this leads to cross peaks of the opposite sign as the diagonal peak spectrum. Large molecules have a negative NOE and conversely cross peaks with the same sign as the diagonal peak. Interactions change the rotational tumbling times and thus influence the sign of NOE cross peaks. Even transient interactions of a small molecule with a large one lead to a sign change in the spectrum that can be used – besides intermolecular NOEs – to prove an interaction. To compare the apparent molecular sizes, 1D and 2D NOESY spectra of all three guest molecules in aqueous buffer (PBS in D_2O, as defined in

Research Article
doi.org/10.1002/ejoc.202300227

the experimental section) were acquired first in absence of the gelator.

The results indicated that the guests belong to different size regimes on the NMR time scale (Figure 2). Glucose **2** showed positive NOEs, which classifies it as small molecule on the NMR time scale (Figure 2a).

Ciprofloxacin **3** also showed positive NOEs at concentrations below 10 mM (Figure 2b). At concentrations higher than 10 mM oligomerization or aggregation took place, discernible from large and increasing line widths with increasing concentrations (Figure S1a). Apparently, also more than one conformation was present, because 1D spectra showed chemical exchange effects, discernible from the different linewidths at the two magnetic fields (Figure S1b). Sodium cholate **4** in aqueous buffer, finally, had negative NOEs (Figure 2c) and thus, as explained above, belongs to the molecules that appear large on the NMR time scale. Yet, the unitary molecular mass of 430 Da should locate **4** in the small molecule regime (with positive NOE sign, typical for molecules below the size of 800–1000 Da in water). Most likely reason for this inconsistence is self-assembly of the amphiphilic **4** in water into aggregates with effective mass above 1000 Da.

Next, we determined the behavior of the photochromic cyclic dipeptide gelator **1** in aqueous medium. In the absence of light, the gelator isomer *E*-**1** forms mechanically stable hydrogels, which undergo liquefaction upon irradiation with green light and partial isomerization to the metastable *Z*-**1** isomer (see Figure 1a). The NOESY spectra of this material (40 g/L, 4 wt.%) were measured in both forms – gel (>95% *E*-**1**) and liquid (58% *Z*-**1**[17]) – in the absence of cargo molecules. In the gel form, it showed strong negative NOEs in the 2D NOESY (Figure 3a). Upon liquefaction, their intensity diminished, while line widths became sharper (Figure 3b).

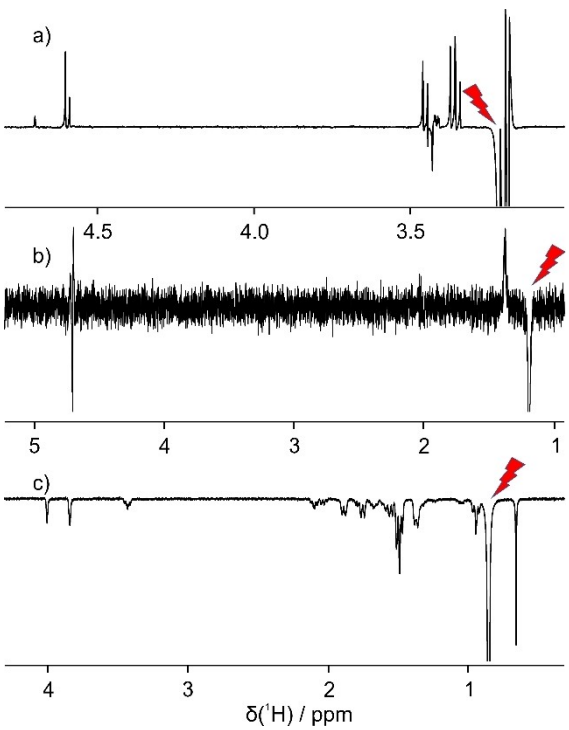

Figure 2. Selective 1D NOESY experiments of a) glucose **2** (40 mM), b) ciprofloxacin **3** (0.5 mM) and c) sodium cholate **4** (40 mM). The irradiation frequency is shown by the red arrow.

Both is a sign that the apparent size of the supramolecular system decreased upon irradiation, which can be explained by the reversible gelation process. As the gel-forming *E*-**1** isomer and the *Z*-**1** isomer with lower self-assembly propensity have slightly altered chemical shifts, we could determine the isomer ratio in the irradiated sample (44% of *E*-**1** and 56% of *Z*-**1**), which is consistent with the previous literature report.[17] These results corroborated with the electron microscopy imaging of the irradiated and non-irradiated material taken at slightly higher concentrations (50 g/L of **1**) – Figure 4a shows extensive cross-linked network of supramolecular fibers in the non-irradiated hydrogel. An irradiated material sample at the same concentration of **1** (Figure 4b) shows strongly reduced fiber network (probably formed from the remaining *E*-**1** molecules), unable to maintain the 3D structure and mechanical stability of the gel. Yet, at even higher concentrations of **1** (>70 g/L or 7 wt.%), the amount of fibers remaining in the irradiated samples is apparently sufficient for the structure stabilization, and the irradiated gels of that concentration do not undergo liquefaction.[17]

NOESY spectra of the cargo molecules inside hydrogels

Then, we analyzed the behavior of hydrogels doped with the three aforementioned cargo substances **2**–**4**. Each of the samples showed a diverse picture.

The 2D NOESY spectrum of glucose **2** encapsulated in the hydrogel showed again negative cross peaks (=positive NOE) of the original glucose signals, stemming from intramolecular contacts (Figure 5). Intermolecular cross peaks between **2** and the gelator **1** were not discernible and chemical shifts were likewise unchanged. The most likely reason for that behavior are strong interactions of polar glucose with the surrounding water molecules, which lead to fluctuating water-glucose hydrogen bonding. The competitive hydrogen bonds between gelator and glucose would have to be strong and static to cause discernable chemical shifts, which is obviously not the case here.

Sodium cholate **4** by itself is a large molecule on the NMR time scale, in the sense defined above. After its encapsulation in the hydrogel, an extensive set of intermolecular cross peaks between **4** and the gelator **1** were observed, along with new intramolecular cross peaks within **4** at 400 ms mixing time (Figure 6). This is probably partially due to spin diffusion, an effect that easily occurs in large systems upon long mixing times. Although intermolecular NOEs have to be generally considered with caution in structural predictions, our results strongly indicate a strong and defined interaction between **4** and **1**. Small modulations (0.05–0.2 ppm) of chemical shifts of the gelator peaks were also observed upon addition of **4**.

Despite some overlap of chemical shifts we could unambiguously identify NOEs of medium strength between the aromatic protons of **1** to methyl groups of **4**: **1**–10/14, **1**–11/13, and **1**–3/

Research Article
doi.org/10.1002/ejoc.202300227

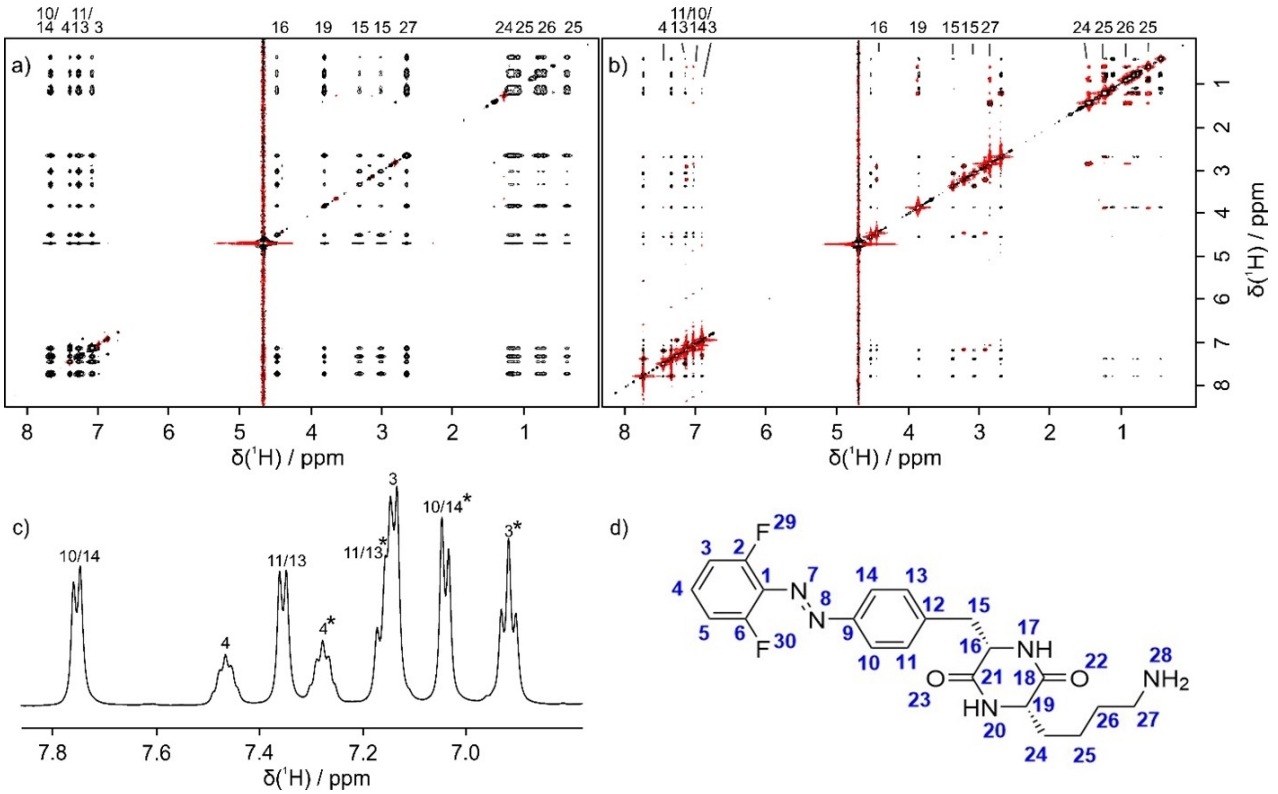

Figure 3. NOESY spectra of the hydrogelator **1**. a) 2D NOESY of the gel composed of *E*-**1**; b) 2D NOESY of the liquid composed from the gel irradiated with green light (majority of the *Z*-**1** isomer, further referred as "switched gelator"); a–b) the red cross peaks (negative phase) originate from the gelator molecules unbound to the supramolecular network, the black cross peaks (positive phase) stem from the gelator bound to the supramolecular network; c) ^{1}H-1D spectrum of the aromatic region of the switched gelator. Peaks with an asterisk belong to the *Z*-**1**, all others stem from the *E*-**1**, d) numbering of atoms of the gelator molecule.

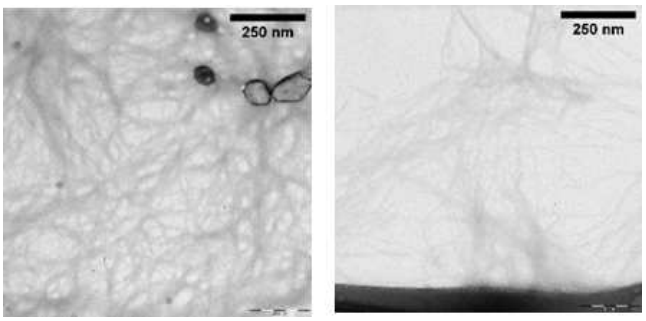

Figure 4. Transmission electron microscopy (TEM) images of the hydrogels – 50 g/L of **1** in PBS buffer – phosphate-buffered saline pH 7.4 (scalebars 250 nm). a) non-irradiated hydrogel; b) irradiation 1 h 523 nm 10 W.

5 (intensities diminish in this order) to **4**–22, **4**–23, and **4**–24, weak NOEs between **1**–10/14 and **1**–11/13 and **4**–12 and **4**–14, weak NOEs between **1**–16 and **4**–23 and **4**–4, **1**–15 to **4**–23 and **4**–4, and very weak NOEs between **1**–19 to **4**–23 and **4**–4, This suggests that the interaction takes place primarily between the hydrophobic side of cholate and the central aromatic ring of the gelator. Hydrogen bonds do not seem to play a significant role, as we already observed for glucose.

Another interesting feature observed in the hydrogel containing cholate **4** as cargo, was its incomplete liquefaction upon irradiation with green light. Furthermore, the irradiated mixture quickly solidified again. Under these conditions, the peak overlap increased even further and we could not unambiguously follow the fate of intermolecular NOE signals in the irradiated samples. In light of our previous discussion regarding self-aggregation of cholate in water (which caused the increase of apparent molecular size above the small-molecule NOE regime for samples containing pure **4** in aqueous medium), we think that the cholate cargo creates non-polar microenvironment that influences the photoconversion efficiency, thermal stability, and the assembly behavior of the gelator **1**, which overall produces the observed macroscopic behavior of the mixture

Ciprofloxacin **3** in its free form has two groups of intramolecular cross peaks: one between protons of the six-membered heterocycle (14–18), and another group within protons that belong to the three-membered cycle (1–3). Both groups of cross peaks have the reverse sign to the diagonal peaks.

After encapsulation of **3** as cargo inside the hydrogel, intramolecular cross peaks between all its hydrogen nuclei could be detected at high concentrations (40 mM of **3**) (Figure S5), but under these conditions they had the same sign as the diagonal peaks. Additionally, several cross peaks between

Research Article
doi.org/10.1002/ejoc.202300227

Chemistry Europe
European Chemical Societies Publishing

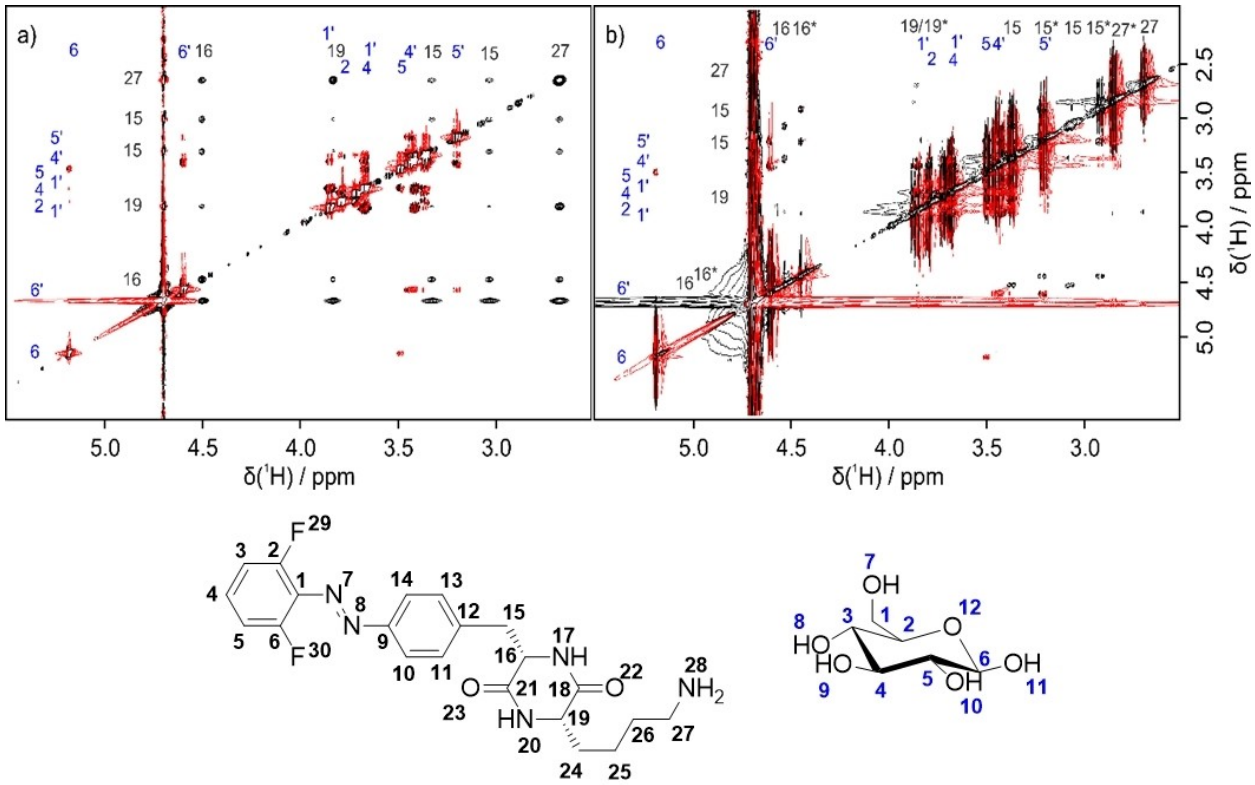

Figure 5. 2D NOESY spectra of the hydrogel loaded with glucose **2** (40 mM), red peaks are the glucose peaks in opposite phase than the gelator **1**. a) non-irradiated hydrogel in darkness, b) hydrogel liquefied with green light (523 nm); Black numbers belong to the gelator, blue numbers to the guest molecule (here, the β-glucopyranose is depicted). The complete spectra – see Figure S3. The blue numbering is used for the β-glucopyranose, and primed numbers are used for the α-glucopyranose structure.

hydrogen atoms of the three-membered ring of ciprofloxacin and the gelator were observed.

In particular, we observed NOEs between **3**-1, **3**-2, **3**-3, and **3**-4 to the aromatic rings of the gelator (Figure 7a and c, numbering is given in Figure 8). They were slightly more intense to **1**–10/14, **1**–11/13 and slightly less intense to **1**–3/5. Also **3**–14/18 of the six-membered heterocycle could show NOEs to the aromatic rings of **1**, but we were not able to unambiguously determine this interaction due to overlap (Figure 7e). It is feasible that also the aromatic hydrogens **3**–9 and **3**–12 interact with those of **1**, but due to the low intensity of the intermolecular NOEs with respect to the intramolecular ones and some overlap we could not unambiguously identify them (Figure 7a).

As **3** at that concentration showed signs of large aggregates in phosphate buffer in the absence of hydrogelator (Figure S1), we were not able to decide a priori whether the cross peaks observed above were a robust sign of interaction with the gelator. We therefore repeated the measurements at lower concentration of **3** (0.5 mM) to verify that the sign change was not simply due to aggregation. Chemical shifts and NOE crosspeaks of ciprofloxacin, including their sign, were essentially identical at low and at high concentration – compare top panels of the Figure S5 and Figure S6. Due to high spectral overlap, only the intramolecular NOEs of the six-membered ciprofloxacin heterocycle could be unambiguously assigned. These showed the same (positive) phase as the gelator cross peaks (Figure 7e and Figure 7g). This is a clear proof that **3** now moved to the large molecule side on the NMR time scale due to the interaction with the gelator irrespective of its self-aggregation in aqueous solution.

To see whether that effect was specific for the gelated form of the material, we measured 2D NOESY spectra once more after its irradiation by green light and liquefaction (Figures S5–S6 *bottom* and right-hand-side panels of the Figure 7). Although the sample was macroscopically fluid, residual resonances and NOE cross peaks of the non-switched gelator were still present – consistent with the microscopic image from Figure 4 and the previously determined photoconversion of 56–58%. Moreover, the two discernible intramolecular cross peaks in **3** could be detected (blue circles, Figure S6). Since they did not change sign, this was an indication that **3** still interacted with **1** (gelator molecules) – otherwise these signals should become negative in phase (Figure S6). They were still visible despite a comparably low concentration of the residual *E*-**1** isomer, because the supramolecular gelator network formed by that isomer has a more efficient NOE transfer (internal as well as to associated molecules) than monomeric *Z*-**1** or monomeric *E*-**1**, and thus becomes more prominent in the spectrum.

At higher cargo concentration (40 mM of **3**) we could not detect any intermolecular cross peaks between gelator and ciprofloxacin after liquefaction (Figure S5). Most of the cross

Research Article
doi.org/10.1002/ejoc.202300227

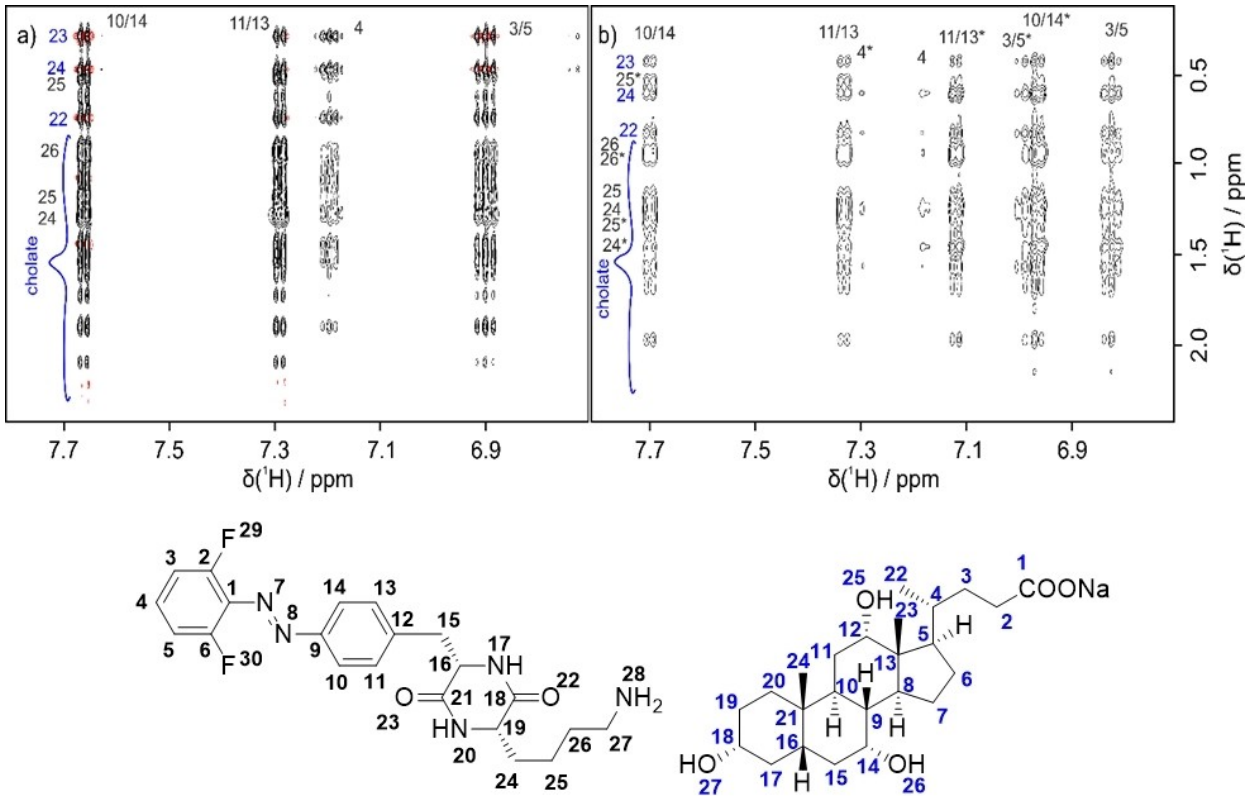

Figure 6. 2D NOESY spectra of the hydrogel loaded with sodium cholate **4** (40 mM). a) non-irradiated hydrogel in darkness, b) hydrogel liquefied with green light (523 nm); interactions between the aromatic region of the gelator **1** and **4** are visible and stronger in the non-irradiated material; Black numbers belong to the gelator, blue numbers to the guest molecule. for the complete spectra – see Figure S4.

peaks of the gelator **1** changed sign, while cross peaks of ciprofloxacin **3** were still positive. In this case, that is probably a sign of self-aggregation of **3** in aqueous buffer, previously observed in the absence of gelator (Figure S1).

DOSY experiments

The DOSY experiment is used to determine the diffusion coefficient of a molecule. Mixtures of two or more molecules are separated in the NMR spectrum according to their diffusion coefficient *D*. We decided to apply this technique to gain additional insight into intramolecular interactions in our materials. We expect that the diffusion coefficient of a guest molecule will become smaller in the case if it measurably interacts with the gelator **1**. However, by interpreting the results we have to be aware that the hydrogel meshwork by itself may lead to a certain reduction of the mean free path length and thus influence the *D* value by purely physical inclusion devoid of specific interactions.

The diffusion coefficients of compounds **2**–**4** in free form and after encapsulation in the hydrogel can be found in Table 1.

Consistent with the NOE data, the diffusion coefficient of glucose **2** did not show distinct changes upon encapsulation in the hydrogel, demonstrating the lack of strong interactions between **2** and the gelator **1**, as well as no serious hindrance of its translational or rotational freedom. Ciprofloxacin **3** and sodium cholate **4**, on the other hand, both exhibited significantly reduced diffusion coefficients upon encapsulation into the hydrogel, indicating that the interactions with **1** restrict their motion.

Table 1. Diffusion coefficients of free cargo substances **2**–**4** compared with the same substances encapsulated in the hydrogel in darkness and upon irradiation (in the fluid samples), as well as the values for gelator **1** in the gel and sol state.

	Free [* 10^{-10} m^2/s]	gel in darkness [* 10^{-10} m^2/s]	Irradiated gel [* 10^{-10} m^2/s]
2	5.2 ± 0.006	4.7 ± 0.006	4.8 ± 0.004
3	4.3 ± 0.05 (0.5 mM)	2.3 ± 0.001	2.7 ± 0.003
4	1.9 ± 0.003	1.2 ± 0.001	1.2 ± 0.006
1	n.a.	3.0 ± 0.007	3.3 ± 0.005

Conclusions

To conclude, we have demonstrated using advanced NMR techniques, that the cargo encapsulation process in supramolecular hydrogels constructed from azobenzene-decorated cyclic dipeptides is driven overwhelmingly by specific guest-gelator supramolecular interactions, and only in minor

Research Article
doi.org/10.1002/ejoc.202300227

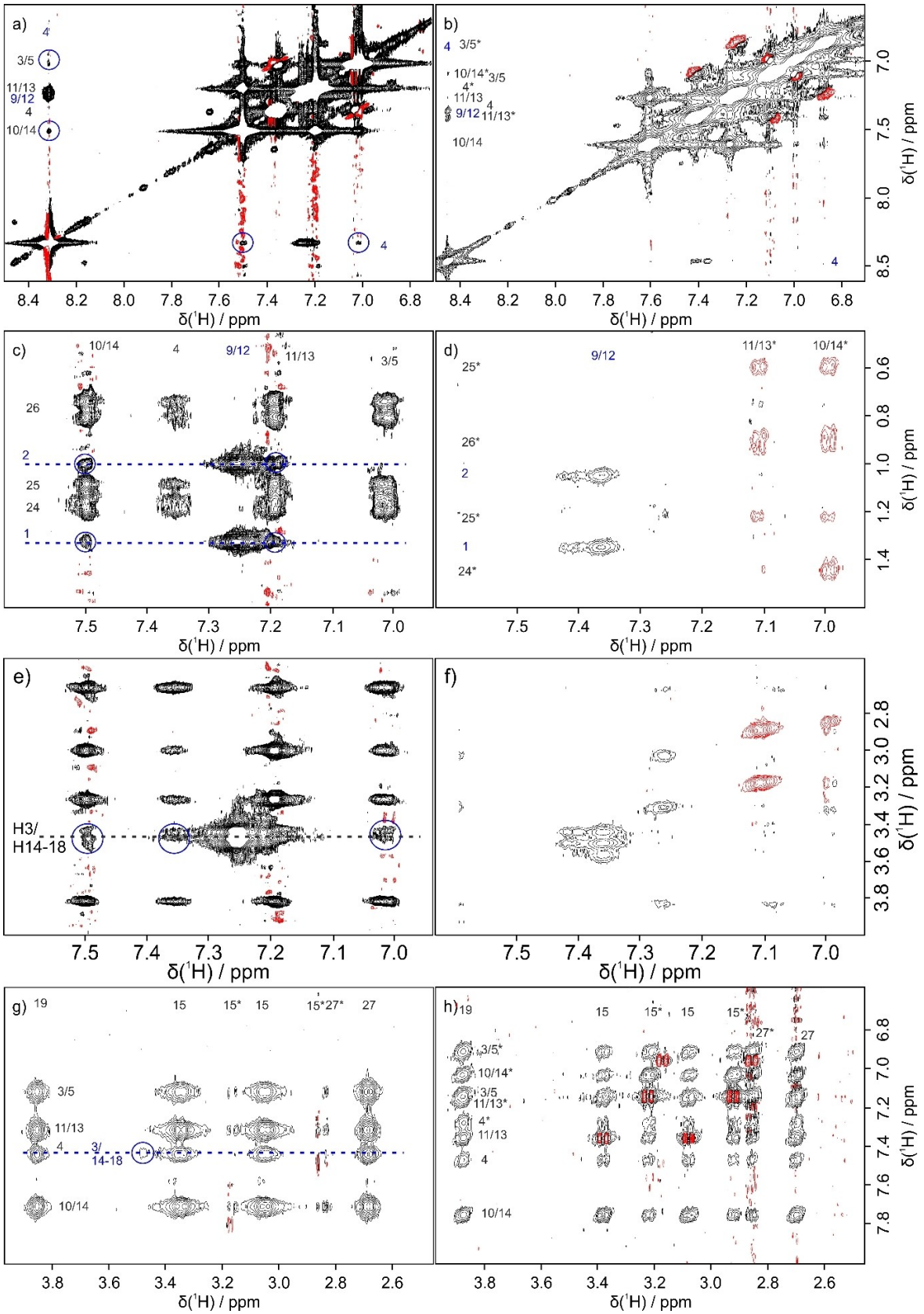

Figure 7. 2D NOESY spectra of the hydrogel loaded with ciprofloxacin **3** a), c), e), g) non-irradiated hydrogel in darkness, b), d), f), h) hydrogel liquefied with green light (523 nm); a)-f) 40 mM of **3** (5×lower base level than full spectra in the Figure S5) g)–h) 0.5 mM of **3** (10x lower base level than full spectra in the Figure S6). Blue circles show the intermolecular interactions between **3** and the gelator **1**. Numbering – see Figure 8 (Black numbers belong to the gelator, blue numbers to the guest molecule). The complete spectra – see Figures S5–S6.

Research Article
doi.org/10.1002/ejoc.202300227

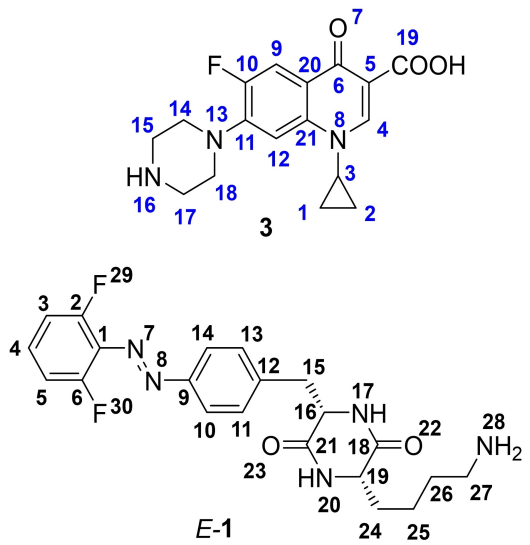

Figure 8. Numbering of atoms in **3** and **1** used for the description of supramolecular and intramolecular interactions observed by NOESY NMR.

part affected by the physical movement restrictions imposed on the cargo by the supramolecular fiber network and the resulting cavities in the volume of the material. The experiments demonstrated above indicate that the specific interactions between the gelator and cargo molecules are primarily of hydrophobic nature. The results of DOSY measurements indicate that the cargo mobility changes are correlated with the apparent specificity of weak host–guest interactions. These observations, supported by our earlier measurements of the leaking rates in darkness for hydrogelator **1** loaded[17] with different cargos, corroborate our empirical hypothesis that the optimal cargo type for our particular gelator structure are molecules with hydrophobic motifs (e.g. aromatic residues) that bear additional acidic groups (like carboxylates) capable of electrostatic interactions with positively charged gelator side chains. Consequently, the hydrogelator design can be optimized towards other cargo of interest. These guidelines, in combination with optimized design of the photoswitch (e.g. red-light-triggered chlorinated azobenzenes that can be switched deep inside human tissues) and proper formulation should provide therapeutically relevant and practically applicable drug delivery compositions with the photorelease mechanism, with minimization of the unwanted leaking process in darkness.

Following the guidelines, an optimal hydrogelator for basic cargo molecules would be a photochromic dipeptide decorated with acidic side chains, which can be synthesized for example by replacing the current lysine fragment with glutamic or aspartic acid. Our preliminary investigation of an analogue of **1** with inverted electrostatic affinity (an azobenzene-bearing cyclic dipeptide with carboxylic acid side chain derived from glutamic acid, instead of the original basic lysine side chain) showed, that this compound failed to form stable hydrogels in neutral aqueous solutions, and thus the inverted charge design needs further optimization. Another, more successful electrostatic stabilization approach was demonstrated by us recently by mixing a hydrogelator bearing lysine side chain with polyanionic covalent alginate.[18] Yet another strategy, however limited to specific type of cargo, is to encapsulate compounds with high structural similarities to the gelator molecule (e.g. potent antimitotic agent plinabulin[19]). Such mixtures show negligible cargo leaking in darkness, probably because the guest molecules incorporate as dopants into the hydrogel fibers.

Experimental Section

Preparation of the gel samples

To a 1.5 mL-vial (crimp top, 12×32 mm) was added 20 mg of the hydrogelator **1** (and optionally the additives **2**, **3**, or **4**) as powder, and 500 μL of the phosphate-buffered saline (PBS) in deuterated water (composition of the PBS buffer: 80 mg NaCl, 2 mg KCl, 14.2 mg Na_2HPO_4 and 2.7 mg KH_2PO_4 in 10.0 mL of D_2O, titrated to the pH ^7.4). This suspension was treated by ultrasonic waves for 2 min followed by heating to 80 °C in a vial block. After equilibration at 80 °C for 5 min, the sample was heated to the boiling point by a heat gun. The hot solution became completely clear and after cooling to ca. 80 °C the sample was transferred to the NMR tubes. Samples were stored in a dark place ready to use.

NMR measurements

Thrippleton-Keeler z-filtered 1D and 2D ^{1}H NOESY spectra (*noesygpphzs)* were acquired at 27 °C on a 600 MHz Bruker Avance III spectrometer equipped with a cryo-TCI probehead (^{1}H, ^{13}C, ^{15}N) with z-gradient (Bruker BioSpin GmbH, Rheinstetten, Germany). Spectra were measured with 16384 data points in the direct dimension, 900 increments, and 16 scans per increment. A mixing time of 400 ms was used.

Selectively refocused 1D NOESY spectra with Thrippleton-Keeler z-filter (*selnogpzs.2*) were measured with 32768 data points and 512 scans.

Additional 1D spectra and DOSY spectra were acquired at 27 °C on a 400 MHz Bruker Avance III HD spectrometer with a BBI room temperature probehead (Bruker BioSpin GmbH, Rheinstetten, Germany). The DOSY pulse sequence was a convection compensated double stimulated echo DOSY(*dstebpgp3s* with corrected delay durations) sequence with 16384 data points and 32 different gradient strengths. Gradient length used and diffusion times are shown in Table S1.

Spectra were multiplied with an exponential window function prior to Fourier transformation in Topspin4.0 (Bruker BioSpin GmbH, Rheinstetten, Germany).

Acknowledgements

The authors gratefully acknowledge the financial support from Deutsche Forschungsgemeinschaft (DFG) – the grants PI 1124/6-3, GRK 2039/1 (Z.P.), SFB1527 HyPERiON C01 (B.L.), YIN Grant of KIT Karlsruhe (Z.P.), the Land of Baden-Württemberg for the support in form of "Landesgraduiertenstipendium" (A.-L. L.) and the Promotionsstipendium from Jürgen Manchot Stiftung (S.K.). C.M.-

G. and B.L. acknowledge support by the Helmholtz society – the HGF-programme Information (43.35.02) and VirtMat. We are indepted to Anna Sonnefeld and Dr. Thomas Gloge for initial experiments. The authors gratefully acknowledge the infrastructural support of our research by Prof. Dr. Stefan Bräse (KIT Karlsruhe) and Prof. Dr. Ute Schepers (KIT Karlsruhe). We also acknowledge support by the KIT Publication Fund of the Karlsruhe Institute of Technology. Open Access funding enabled and organized by Projekt DEAL.

Conflict of Interests

The authors declare no conflict of interest.

Data Availability Statement

The data that support the findings of this study are available in the supplementary material of this article.

Keywords: azobenzene · DOSY · NOESY · photochromic materials · supramolecular hydrogels

[1] a) F. Farjadian, S. Ghasemi, M. Akbarian, M. Hoseini-Ghahfarokhi, M. Moghoofei, M. Doroudian, *Front. Chem.* **2022**, *10*, 952675; b) Y. Lu, W. Sun, Z. Gu, *J. Controlled Release* **2014**, *194*, 1–19; c) M. Vicario-de-la-Torre, J. Forcada, *Gels* **2017**, *3*, 16.

[2] a) J. E. Yap, L. Zhang, J. T. Lovegrove, J. E. Beves, M. H. Stenzel, *Macromol. Rapid Commun.* **2020**, *41*, 2000236; b) C. S. Linsley, B. M. Wu, *Ther. Delivery* **2017**, *8*, 89–107; c) X. Ai, J. Mu, B. Xing, *Theranostics* **2016**, *6*, 2439–2457; d) A.-L. Leistner, Z. L. Pianowski, *Eur. J. Org. Chem.* **2022**, *2022*, e202101271.

[3] a) Z. L. Pianowski, *Chem. Eur. J.* **2019**, *25*, 5128–5144; b) J. Volarić, W. Szymanski, N. A. Simeth, B. L. Feringa, *Chem. Soc. Rev.* **2021**, *50*, 12377–12449; c) M.-M. Russew, S. Hecht, *Adv. Mater.* **2010**, *22*, 3348–3360; d) A. Goulet-Hanssens, F. Eisenreich, S. Hecht, *Adv. Mater.* **2020**, *32*, 1905966.

[4] P. Klán, J. Wirz, in *Molecular Photoswitches*, (Ed. Z. Pianowski) Wiley-VCH, Weinheim, Germany **2022**, pp. 1–18.

[5] H. Bouas-Laurent, H. Dürr, *Pure Appl. Chem.* **2001**, *73*, 639–665.

[6] a) H. M. D. Bandara, S. C. Burdette, *Chem. Soc. Rev.* **2012**, *41*, 1809–1825; b) S. Crespi, N. A. Simeth, B. König, *Nat. Chem. Rev.* **2019**, *3*, 133–146; c) V. Koch, S. Bräse, in *Molecular Photoswitches*, (Ed. Z. Pianowski) Wiley-VCH, Weinheim, Germany **2022**, pp. 39–64.

[7] a) M. Irie, T. Fukaminato, K. Matsuda, S. Kobatake, *Chem. Rev.* **2014**, *114*, 12174–12277; b) I. V. Komarov, S. Afonin, O. Babii, T. Schober, A. S. Ulrich, in *Molecular Photoswitches*, (Ed. Z. Pianowski) Wiley-VCH, Weinheim, Germany **2022**, pp. 151–175.

[8] a) L. Kortekaas, W. R. Browne, *Chem. Soc. Rev.* **2019**, *48*, 3406–3424; b) R. Klajn, *Chem. Soc. Rev.* **2014**, *43*, 148–184; c) L. Kortekaas, W. R. Browne, in *Molecular Photoswitches*, (Ed. Z. Pianowski) Wiley-VCH, Weinheim, Germany **2022**, pp. 131–149.

[9] a) J. D. Harris, M. J. Moran, I. Aprahamian, *Proc. Natl. Acad. Sci. USA* **2018**, *115*, 9414–9422; b) D. Cameron, S. Eisler, *J. Phys. Org. Chem.* **2018**, *31*, e3858.

[10] a) B. Shao, I. Aprahamian, *Chem* **2020**, *6*, 2162–2173; b) I. Aprahamian, *Chem. Commun.* **2017**, *53*, 6674–6684.

[11] C. Petermayer, H. Dube, *Acc. Chem. Res.* **2018**, *51*, 1153–1163.

[12] M. M. Lerch, W. Szymański, B. L. Feringa, *Chem. Soc. Rev.* **2018**, *47*, 1910–1937.

[13] a) S. Kirchner, A.-L. Leistner, P. Gödtel, A. Seliwjorstow, S. Weber, J. Karcher, M. Nieger, Z. Pianowski, *Nat. Commun.* **2022**, *13*, 6066; b) P. Gödtel, J. Starrett, Z. Pianowski, *Chem. Eur. J.* **2023**, *29*, e202204009.

[14] a) E. R. Draper, D. J. Adams, *Chem. Commun.* **2016**, *52*, 8196–8206; b) Z. Qiu, H. Yu, J. Li, Y. Wang, Y. Zhang, *Chem. Commun.* **2009**, *23*, 3342–3344; c) C.-W. Chu, B. J. Ravoo, *Chem. Commun.* **2017**, *53*, 12450–12453; d) B. P. Nowak, B. J. Ravoo, *Soft Matter* **2020**, *16*, 7299–7304.

[15] L. Li, J. M. Scheiger, P. A. Levkin, *Adv. Mater.* **2019**, *31*, 1807333.

[16] a) Z. L. Pianowski, J. Karcher, K. Schneider, *Chem. Commun.* **2016**, *52*, 3143–3146; b) A.-L. Leistner, S. Kirchner, J. Karcher, T. Bantle, M. L. Schulte, P. Gödtel, C. Fengler, Z. L. Pianowski, *Chem. Eur. J.* **2021**, *27*, 8094–8099.

[17] J. Karcher, Z. L. Pianowski, *Chem. Eur. J.* **2018**, *24*, 11605–11610.

[18] A.-L. Leistner, D. G. Kistner, C. Fengler, Z. L. Pianowski, *RSC Adv.* **2022**, *12*, 4771–4776.

[19] J. Karcher, S. Kirchner, A.-L. Leistner, C. Hald, P. Geng, T. Bantle, P. Gödtel, J. Pfeifer, Z. L. Pianowski, *RSC Adv.* **2021**, *11*, 8546–8551.

[20] S. M. Ramalhete, K. P. Nartowski, N. Sarathchandra, J. S. Foster, A. N. Round, J. Angulo, G. O. Lloyd, Y. Z. Khimyak, *Chem. Eur. J.* **2017**, *23*, 8014–8024.

[21] R. Van Lommel, J. Van Hooste, J. Vandaele, G. Steurs, T. Van der Donck, F. De Proft, S. Rocha, D. Sakellariou, M. Alonso, W. M. De Borggraeve, *Gels* **2022**, *8*, 813.

[22] M. J. Clemente, P. Romero, J. L. Serrano, J. Fitremann, L. Oriol, *Chem. Mater.* **2012**, *24*, 3847–3858.

[23] Y. Che, J. Gaitzsch, N. Liubimtsev, S. Zschoche, T. Bauer, D. Appelhans, B. Voit, *Soft Matter* **2020**, *16*, 6733–6742.

[24] A. Ziéba, A. Maślankiewicz, J. Sitkowski, *Magn. Reson. Chem.* **2004**, *42*, 903–904.

[25] J. C. Hoch, K. Baskaran, H. Burr, J. Chin, Hamid R. Eghbalnia, T. Fujiwara, Michael R. Gryk, T. Iwata, C. Kojima, G. Kurisu, D. Maziuk, Y. Miyanoiri, Jonathan R. Wedell, C. Wilburn, H. Yao, M. Yokochi, *Nucleic Acids Res.* **2022**, *51*, D368–D376.

Manuscript received: March 11, 2023
Revised manuscript received: April 21, 2023
Accepted manuscript online: April 24, 2023